ELSEVIER

Polymer 42 (2001) 5199–5205

polymer

www.elsevier.nl/locate/polymer

Miscibility, crystallinity and morphological behavior of binary blends of poly(ethylene oxide) and poly(methyl vinyl ether–maleic acid)

A.M. Rocco[a,*], R.P. Pereira[a], M.I. Felisberti[b]

[a]*Instituto de Química, Universidade Federal do Rio de Janeiro, Cidade Universitária, CT, Bloco A,*
221949-900 Rio de Janeiro, RJ, Brazil
[b]*Instituto de Química, Universidade Estadual de Campinas, Campinas, São Paulo, Brazil*

Received 17 February 2000; received in revised form 20 September 2000; accepted 22 October 2000

Abstract

DSC and optical microscopy were used to determine the miscibility and crystallinity of blends of poly(ethylene oxide) (PEO) with poly(methyl vinyl ether–*co*–maleic acid) (PMVE–MAc). Single T_g was observed for all blends, indicating miscibility. The dependence of T_g on the weight per cent of PEO presents a negative deviation from linearity at high PEO content, associated to a greater blend free volume, mobility and flexibility than in pure PEO. A progressive decrease in the degree of crystallinity and in the size of the PEO spherullites as the PMVE–MAc is added is observed. FTIR provided evidence of specific interaction between the polymers. © 2001 Elsevier Science Ltd. All rights reserved.

Keywords: Blends; Miscibility; PEO

1. Introduction

Polymer solid electrolytes (PSE) are materials of great technological interest because of their applications in solid state batteries [1], capacitors [2,3] and electrochromic devices [4]. The polymer electrolyte materials are characterized by an interesting conductivity behavior that is highly dependent on the local structure and is influenced by crystallization and ionic association. Among the first [1] and most studied polymers in PSE is PEO, due to the fact that it easily dissolves alkali metal salts. However, PEO possesses ionic conduction appreciable only above 65°C [5]. At temperatures below 65°C, PEO–salt electrolytes consist of mixtures of spherullite crystalline phases separated by amorphous solutions of salt in PEO and ion conduction takes place primarily in the amorphous regions [6–8].

One of the methods to improve the conductivity of PEO-based electrolytes is modification of the polymer matrix by incorporation of plasticizers to make the matrix more liquid-like. The addition of small molecules such as PEO oligomers, ethylene carbonate and propylene carbonate as plasticizers facilitates long chain segmental motion. However, a serious disadvantage is that most plasticizers are volatile at room temperature, leading to their loss from the samples [9]. Efforts to enhance the ionic conductivity of the solid electrolytes based on PEO focused on suppressing its crystallization, via incorporating compounds with low T_g [10] and by copolymerization of PEO with macromonomers [11]. Copolymerization is a way to lower the melting point, modulus as well as crystallinity and to increase solubility and transparency [12]. Possible alternatives are grafting [13] and cross-linking [14]. Although these novel approaches are promising, the fact that their preparation requires nontrivial synthetic processes is a serious drawback to practical applications. It is of considerable importance to develop an easier method for preparing the polymer electrolytes with higher ionic conductivities and dimensional stability. In this regard, recent works on the preparation of polymer electrolytes by blending polymers are of interest [15–18]. Blending polymers is an economic and quick alternative for obtaining materials with optimized properties. The main advantages of these blend-based systems are simplicity of preparation and easy control of physical properties by compositional change. Much work has been done on binary PEO-based blends, where the second component is non-crystalline and is able to inhibit crystallization of the PEO [19,20]. By blending, thermal, mechanical, and adhesive properties associated with high transparency can be optimized, depending on the non-crystalline polymer. These properties are desired for applications in devices. They are optimized by deposition, by casting on the electrodes. The

---

[*] Corresponding author. Fax: + 55-21-5627559.
E-mail address: amrocco@iq.ufrj.br (A.M. Rocco).

0032-3861/01/$ - see front matter © 2001 Elsevier Science Ltd. All rights reserved.
PII: S0032-3861(00)00784-9

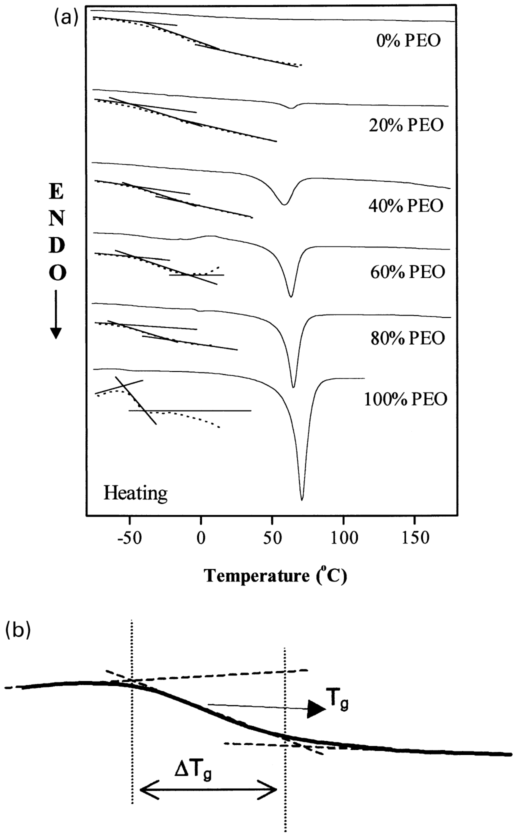

Fig. 1. (a) DSC curves for PEO/PMVE–MAc blends recorded at a heating rate of 20°C/min. (b) Schematic plot for the determination of Tg and (1Δ)Tg.

casting method allows one to obtain PSE films less than 10 μm thick, which diminishes the time response for these devices [4].

Another important consideration in the choice of blend components is the intermolecular interaction, which are considered to play a key role in polymer miscibility. It has been well reported [21,22] that PEO, because of its basic oxygen, is a good proton-accepting polymer, which permits a hydrogen-bonding interaction in a blend with a proton-donor polymer.

This work is part of the study and development by our group of new hosts for PSE based on PEO, with its crystallinity reduced by blending or obtaining nanocomposites. In this study we investigate the miscibility of a binary blend based on PEO and PMVE–MAc. The second polymer can 'self-associate' (i.e. is hydrogen bonded in the pure state) and is capable of hydrogen bonding to the basic oxygen [23] of PEO.

2. Experimental section

2.1. Materials

The poly(methyl vinyl ether–maleic acid), PMVE–MAc ($M_w = 1.910^6$ g/mol) and PEO ($M_w = 4.10^6$ g/mol) were supplied by Aldrich Chem. Co. and utilized without further purification.

2.2. Sample preparation

PEO and PMVE–MAc with ratios of 100/0, 80/20, 60/40, 40/60, 20/80 and 0/100 wt% were dissolved in methanol (Merck, PA). The solution was stirred for 8 h. Films were prepared by casting from these solutions onto pre-heated glass plates and dried until constant weight in a dessicator under vacuum.

2.3. Differential scanning calorimetry (DSC)

To evaluate the miscibility and thermal behavior of the blends, DSC measurements were performed on a General V4.1C DuPont 2100 apparatus. The apparatus was calibrated with an indium standard under nitrogen atmosphere.

Samples were first heated from 25 to 150°C at a heating rate of 20°C/min (run I). After a 5 min isotherm, samples were then cooled to -100°C at the same rate (run II) and then heated at 20°C/min to 100°C (run III). The melting temperatures (T_m) and apparent melting enthalpy (ΔH_m) were determined from the DSC endothermic peaks on the second heating run. Glass transition temperatures, T_g, were estimated as the onset temperature. The melting enthalpies and temperatures were derived from the area and the maximum of the endothermic peaks, respectively. The degree of crystallinity was calculated from the following equations:

$$\chi_c(\text{blend}) = \frac{\Delta H_{\text{m,blend}}}{\Delta H^{\text{o}}_{\text{PEO}}} \tag{1}$$

$$\chi_c(\text{PEO}) = \frac{\Delta H_{\text{m,PEO}}}{\Delta H^{\text{o}}_{\text{PEO}}} \tag{2}$$

where $\Delta H_{\text{m,blend}}$ and $\Delta H_{\text{m,PEO}}$ are the apparent melting enthalpies per gram of blend and of PEO present on the blend, respectively, and $\Delta H^{\text{o}}_{\text{PEO}}$ is the heat of melting per gram of 100% crystalline PEO, 188 J/g [24].

2.4. Morphological studies

After 15 days the samples deposited on glass plates were analyzed by optical microscopy in an Olympus BX-50, with crossed polars.

2.5. Fourier transform infrared spectroscopy (FTIR)

For the FTIR measures, samples were prepared by casting directly onto NaCl pellets and films dried under vacuum. FTIR spectra were obtained on a Nicolet-760 FTIR spectrometer at room temperature. One hundred and twenty-eight scans were taken with a resolution of 1 cm^{-1} and gain of 2.0 for all samples.

Table 1
Thermal properties of PEO/PMVE–MAc blends

% PEO	T_g (°C)	ΔT_g (°C)	T_m (°C)	$\Delta H_{m,blend}$ (J/g)	$\Delta H_{m,PEO}$ (J/g)	$\chi_{c(PEO)}$ (%)
0	−9	76	–	–	–	–
20	−20	55	64	7	35	19
40	−26	46	58	26	65	35
60	−29	32	63	57	95	51
80	−37	36	65	93	116	62
100	−45	15	72	136	136	72

3. Results and discussion

3.1. DSC

The blends prepared as described above were transparent including those richer in PEO. Blends presented more elasticity than pure PEO and adhered well to the glass. These properties are desirable for application in PSE. The DSC curves are shown in Fig. 1a, where the amplified glass transition temperature is evident. In Table 1 the glass transition temperature, glass transition width (ΔT_g), melting temperature, $\Delta H_{m,blend}$, $\Delta H_{m,PEO}$ and crystallinity degree, χ_c, for all samples are shown.

Only one glass transition temperature can be observed for all the samples, which indicates miscibility within the limits of detection of the DSC technique. The glass transition width for the samples richer in PMVE–MAc attain higher values, as can be observed in Table 1.

Glass transition width (ΔT_g), is defined as the difference between onset and endset of the glass transition process, as illustrated in Fig. 1b. ΔT_g reflects the number of relaxation processes associated with the glass transition. If the system exhibits microenvironments caused by dipole–dipole interactions, or hydrogen bonding, then this should undergo relaxation processes with different relaxation times, resulting in broadening of the glass transition.

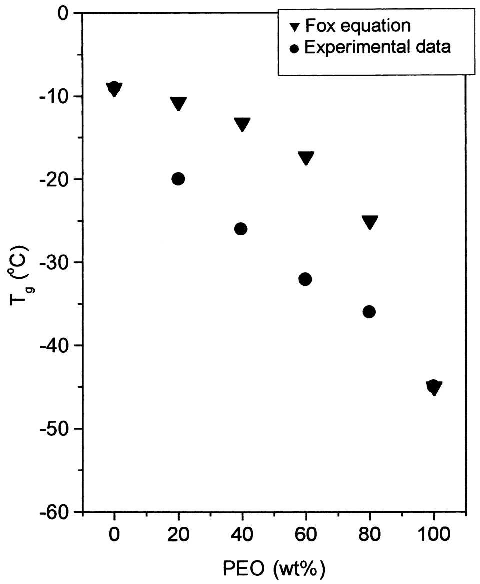

Fig. 2. Dependence of T_g (●) of the PEO/PMVE–MAc blends on the weight per cent of PEO. Fox equation prediction (▲).

Values of ΔT_g in the range of 10–30°C are expected for semicrystalline homopolymers, as observed for PEO in Table 1. For PMVE–MAc the value of ΔT_g is 76°C. This may reflect heterogeneities at the molecular level. There may be chain regions richer in ether groups and regions richer in acid groups. These different chain regions should undergo different relaxation times, and this would cause the broadening of the ΔT_g observed. Another factor which could explain the high value of ΔT_g observed for PMVE–MAc would be hydrogen bonding in the intra- or inter-chain arrangement. For samples richer in PMVE–MAc, ΔT_g is observed to attain higher values, which may be associated with the intrinsic characteristics of the copolymer. However, the presence of a broad ΔT_g does not affect the determination of the glass transition temperature of the system.

The Fox Eq. (3) was utilized to describe the dependence of T_g on the composition of the blend (Fig. 2). This is one of the empirical equations that describe the dependence of T_g on the blend composition for miscible systems:

$$\frac{1}{T_g} = \frac{w_A}{T_{g,A}} + \frac{w_B}{T_{g,B}} \qquad (3)$$

where w_A and w_B are the mass percentages and $T_{g,A}$ and $T_{g,B}$ are the glass transition temperatures for A and B polymers, respectively.

It can be seen that the observed T_g increases with the PMVE–MAc composition, and the dependence of the calculated T_g on the blend composition exhibits a positive deviation with respect to linearity. The Fox equation describes the T_g behavior rather poorly, because it is valid only for ideal mixtures, where it is assumed that the homogeneous and heterogeneous interactions are equivalent. For an exothermic mixture, interactions between the two different polymers would be favored. Ideal conditions do not hold in the blend studied here, which can be seen from the strong evidence for miscibility. The experimental data, however, present a negative deviation with respect to linearity, which can be associated with a greater blend free volume, mobility and flexibility than in pure PEO.

In Fig. 3 a decrease of T_m from 72°C for pure PEO to 64°C

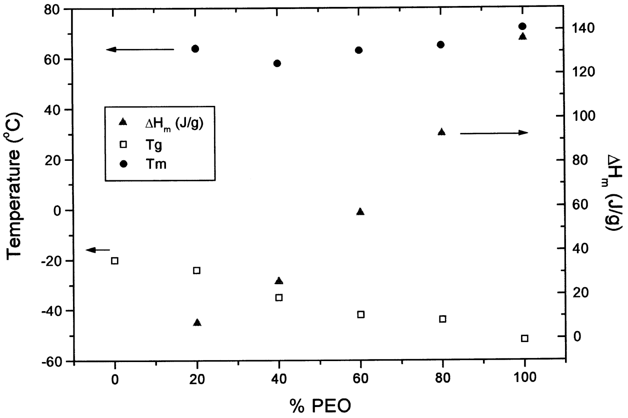

Fig. 3. Dependence of T_g (□), ΔH_m (▲) and T_m (●) of PEO/PMVE–MAc blends, on the weight per cent of PEO.

for blend with 20% PEO can be seen. The melting temperature obtained, most likely, does not correspond to the equilibrium melting temperature but rather reflects morphological aspects (crystal size, defects on the crystalline phase) and also thermodynamic aspects. The morphological aspects are determined by the crystallization kinetics. Despite the influence of morphological analysis, it is evident that the tendency of the lowering of T_m with an increase of PMVE–MAc concentration in the blends indicates miscibility. $\Delta H_{m,PEO}$ decreased from 136 to 35 J/g, and the great decrease of χ_c and T_m (72–58°C from 100 to 40% PEO) with PMVE–MAc addition are consistent with what has been observed for non-crystalline/crystalline polymer blends.

The phase diagram for the blend (Fig. 3) shows that above the PEO melting point line a liquid phase is present. Between the PEO T_m and T_g lines, crystals of PEO together with a PEO/PMVE–MAc non-crystalline phase coexist. Below the T_g line, PEO crystalline phases coexist with a glass homogeneous PEO/PMVE–MAc phase. The viscoelastic region of the phase diagram comprehends a great range of temperature, which is necessary for the intended application of this system.

Analysis of the optical photomicrographs (Fig. 4) shows large crystals for the sample containing 100% PEO. A progressive reduction in the size of the crystals can be seen, being more pronounced with higher concentrations of PMVE–MAc. For the samples which contain 40, 20 and 0% PEO, there are no crystals that can be seen with the resolution and magnification utilized.

The results based on DSC and optical microscopy indicate that the crystallinity of the samples is reduced with the addition of PMVE–MAc, which inhibited crystallization, with an obvious modification of the kinetics of crystal formation and a depression of the melting point. This indicated that there is a negative Flory–Huggins interaction parameter (x_{12}) between the two polymer components. The decrease of the melting point of the crystallizable component in miscible blends has been thermodynamically described by Imken et al. [25] and Nish and Wang [26] and indicates that there is a negative interaction parameter (x_{12}) between the polymers.

The decrease of crystallinity changes the composition of the amorphous phase in the blend, which reinforces the explanation for the negative deviation from linearity [27] of the experimental T_g data.

3.2. FTIR

From the DSC studies it has been concluded PEO/PMVE–MAc blends are miscible. It has been reported [21,22] that PEO, because it is an ether, is a good proton-accepting polymer which makes hydrogen bonding possible

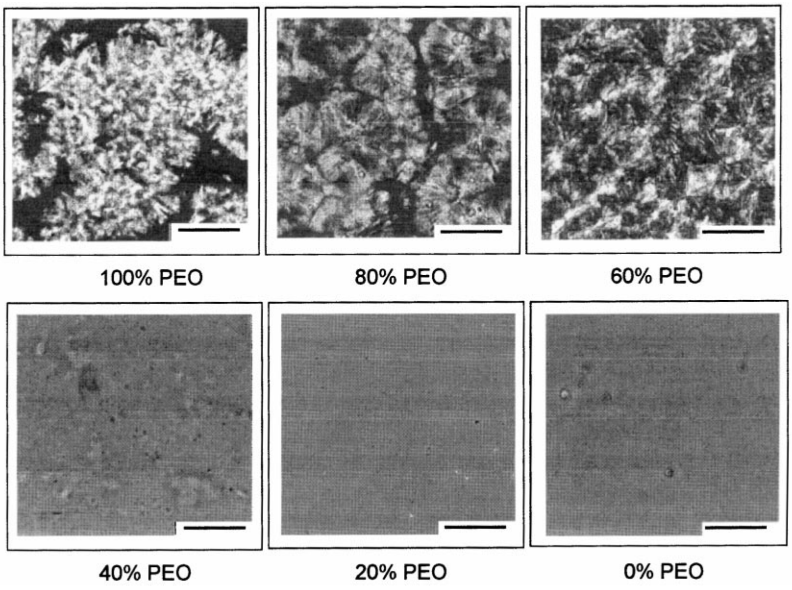

Fig. 4. Optical photomicrographs of the blends PEO/PMVE–MAc. Bar represents 50 mm.

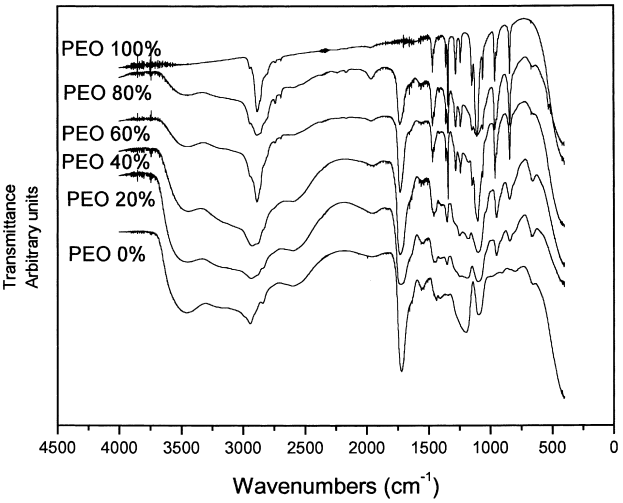

Fig. 5. FTIR spectra of pure PEO, pure PMVE–MAc and PEO/PMVE–MAc blends.

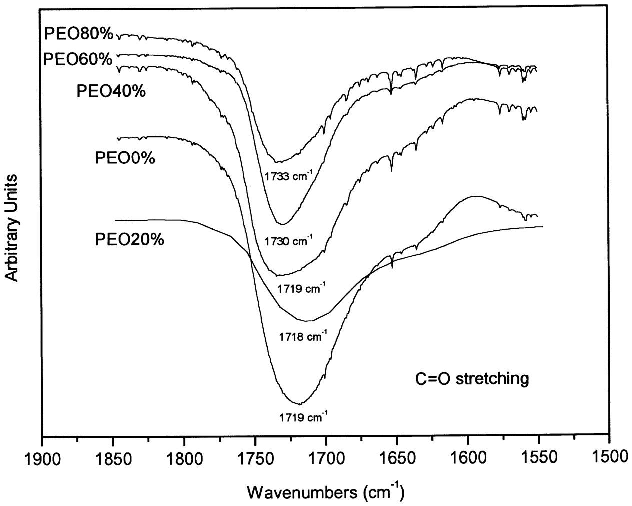

Fig. 7. FTIR spectra in the carbonyl group region for pure PMVE–MAc and PEO/PMVE–MAc blends.

in a blend of PEO and a proton-donating polymer. The polymer used in this work presents O–H acid groups as a proton donor and can play an important role in the miscibility of PEO/PMVE–MAc blends.

Fig. 5 shows the FTIR spectra for pure polymers and for the blends in the compositions studied. The hydroxyl region is not as easily amenable for quantitative evaluation because of vibrational overlap and possible changes in absorption coefficients and frequencies of free, self- and inter-associated (Fig. 6a and b) O–H components [28]. However, pure PMVE–MAc presents a carbonyl group yielding, a ν(C=O) stretching mode centered at 1719 cm^{-1} with a shoulder from 1600 to 1650 cm^{-1}, probably due to the contributions of free and bound C=O, respectively. The carbonyl stretching bands, as a function of composition for the blends, are shown in Fig. 7. When blending PMVE–MAc with PEO, it is clear the decrease in shoulder intensity, probably due to the decrease of the concentration of bound carbonyl groups. At the same time it can be seen that the peak maximum shifts to higher wavenumbers. At 80% PEO a ν(C=O) stretching mode is centered at 1733 cm^{-1}. Probably the O–H groups of PMVE–MAc form hydrogen bonds with the basic oxygen atoms of PEO, freeing C=O groups which were previously involved in intramolecular hydrogen bonds, which results in the solubility and dilution of PMVE–MAc in PEO.

In Fig. 8 the spectra in the range of 1220–980 cm^{-1} of pure PEO and the blends 80 and 60% PEO are shown. A crystalline PEO phase is confirmed by the presence of the triplet peak of the C–O–C stretching vibration at 1149, 1109, and 1061 cm^{-1} with maximum at 1109 cm^{-1} [29,30]. Changes in the intensity, shape, and position of the C–O–C stretching mode are associated with the interaction between PEO and PMVE–MAc. The decrease in the position of the C–O–C stretching maximum can be noted

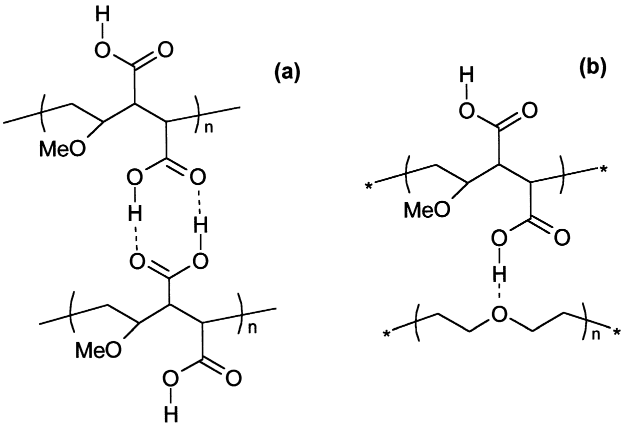

Fig. 6. Schematic structure for hydrogen bond interactions between: (a) PMVE–MAc/PMVE–MAc, and (b) PEO/PMVE–MAc molecules.

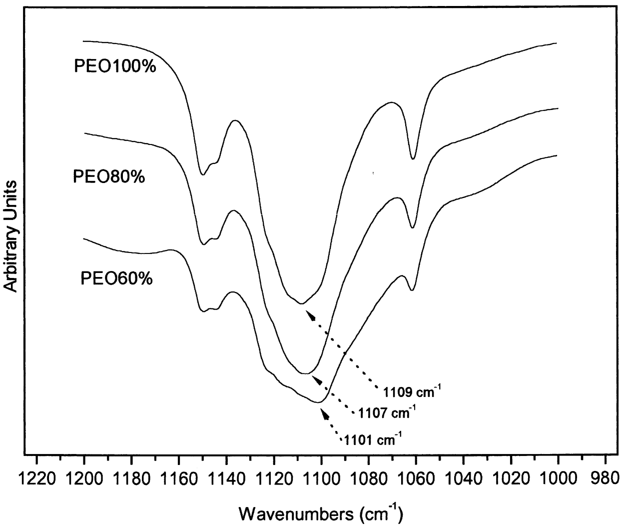

Fig. 8. FTIR spectra recorded for pure PEO and for 80 and 60 wt% PEO in the frequency range from 1220 to 1000 cm^{-1}.

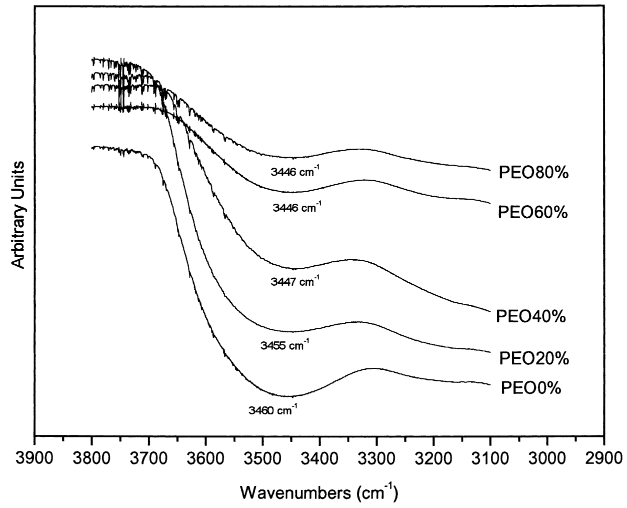

Fig. 9. FTIR spectra in the hydroxyl group region for pure PMVE–MAc and PEO/PMVE–MAc blends.

with an increase in the PMVE–MAc concentration. For 60% PEO the stretching mode C–O–C lies at 1101 cm^{-1}. The broadening of this band, particularly at the highest PMVE–MAc content, is also observed. The intensity of the peaks at 1144 and 1062 cm^{-1} decrease, probably due to the decrease of PEO crystallinity in the blends, as observed in the calculated degree of crystallinity. These results indicate that the intermolecular hydrogen bonding between the ether oxygen and the O–H acid group is formed, which is consistent with the shifts seen previously in the region of C=O stretching in the spectrum of PMVE–MAc.

However, the hydroxyl region is not as easily amenable to quantitative evaluation, in this work a qualitative study of these vibrational mode changes was done, motivated by preliminary studies of the C=O and C–O–C modes. Fig. 9 presents the spectra in the hydroxyl stretching region of the PMVE–MAc and PEO/PMVE–MAc blends. One large vibrational band due to O–H group stretches in pure PMVE–MAc is centered at 3460 cm^{-1}. The band was attributed to the contribution of stretching vibration of 'free' and self-associated O–H hydrogen bonding hydroxyl groups [21]. For pure PMVE–MAc a weak band of the O–H acid group dimer at 1439 cm^{-1} [31] is observed, which justifies the presence of a self-association interaction. In blends with PEO, as this polymer is added, the peak originally at 3460 cm^{-1} shifts gradually to lower wavenumbers reaching 3446 cm^{-1} at 80% PEO. Peak changes indicate that free and self-associated O–H groups are decreasing to the benefit of the formation of inter-associated hydrogen bonds with the PEO basic oxygen at higher PEO compositions [32,33]. O–H groups of PMVE–MAc are probably randomly distributed among an increasing number of C–O–C groups of PEO, statistically favoring the formation of the inter-associated interaction, which is weaker than the other two interactions [21].

At the molecular level, FTIR studies provided strong evidence that there is a specific interaction between the PEO and PMVE–MAc molecules, which favors the miscibility of the blend, at the same time that it can be responsible for the increase in the T_g value.

4. Conclusions

The study of PEO/PMVE–MAc blends using DSC showed single T_g with a value intermediate between both the pure constituents, indicating miscibility. The study of the dependence of T_g on the weight per cent of PEO presents a negative deviation from linearity at high PEO content. This is associated with a greater blend free volume, mobility and flexibility than in pure PEO. The presence of PMVE–MAc in the blends hindered the crystallization of PEO, thus decreasing the calculated degree of crystallinity and size of the PEO spherullites and depressing the melting point of the system. The results presented here clearly show that PEO/PMVE–MAc blends are miscible over the entire range of compositions studied. At the molecular level the miscibility between PEO and PMVE–MAc is mainly attributed to intramolecular hydrogen bonds. From the results obtained, this system is considered a promissory matrix for a PSE.

Acknowledgements

The authors would like to thank CNPq for the fellowships.

References

[1] Acosta JL, Morales E. J Appl Polym Sci 1996;60:1185.
[2] Mastragostino M, Arbizzani C, Meneghelo L, Paraventi R. Adv Mater 1996;4:331.
[3] Rudge A, Davey J, Raistrick I, Gottesfeld S, Ferraris JP. J Power Sources 1994;89:47.
[4] De Paoli M-A, Zanelli A, Mastragostino M, Rocco AM. J Electroanal Chem 1997;435:217.
[5] Bruce PG, editor. Solid state electrochemistry. Cambridge: Cambridge University Press, 1997. p. 106.
[6] Armand MB. In: McCallum JR, Vincent CA, editors. Polymer electrolyte reviews, vol. 1. London: Elsevier Applied Science, 1989. p. 1.
[7] Berthier C, Gorecki W, Minier M, Armand MB, Chabagno JM, Rigaud P. Solid State Ionics 1983;11:91.
[8] Fauteux D, Purd'homme J, Harvey PE. Solid State Ionics 1988;28:923.
[9] Chintapallis FR, Grad B. Polymer 1997;38:6189.
[10] Lee CC, Wright PV. Polymer 1982;23:681.
[11] Xia DW, Smid J. J Polym Sci Polym Lett 1984;22:617.
[12] Zheng S, Huang J, Liu W, Yang X, Guo Q. Eur Polym J 1996;32:757.
[13] Su F, Feng LX, Yang SL. Appl Chem 1987;4:40.
[14] Fish D, Xia DW, Smid S. Makromol Chem 1985;6:761.
[15] Acosta JL, Morales E. Solid State Ionics 1996;85:85.
[16] Kim D-W, Park JK, Rhee H-W. Solid State Ionics 1996;83:49.
[17] Wieczorek W, Such K, Przyluski P, Florjanczyk Z. Synth Met 1990;45:373.
[18] Li J, Khen IM. Macromolecules 1993;26:4544.
[19] Herrero CR, Acosta JL. Polym J 1994;26(7):786.
[20] Cohen LE, Rocco AM. J Therm Anal Cal 2000;59:625.

[21] Coleman MKM, Moskala EJ. Polymer 1983;24:251.

[22] Berridi MJF, Valero M, Learthum AM, Espi E, Truin J. Polymer 1994;34:38.

[23] Coleman MM, Graf JF, Painter PC. Specific interactions and the miscibility of polymer blends. Lancaster, PA: Technomic Publishing, 1991.

[24] Cimmino S. Makromol Chem 1990;19:2447.

[25] Imken RL, Paul DR, Barlow JW. Polym Engng Sci 1976:16,593.

[26] Nish T, Wang TT. Macromolecules 1975;18:909.

[27] Zheng S, Huang J, Liu W, Yang X, Guo Q. Eur Polym J 1996;32:757.

[28] Li D, Brisson J. Polymer 1998;39:793.

[29] Li X, Hsu SL. J Polym Sci Polym Phys Ed 1984;22:1331.

[30] Bailey Jr. FE, Koleske JV. Poly(ethylene oxide). New York: Academic Press, 1976 (p. 115).

[31] Pavia DL, Lampman GM, Kriz GS. Introduction to spectroscopy. 2nd ed. New York: Saunders College Publishing, 1996 (p. 461).

[32] Purcell KF, Drago RS. J Am Chem Soc 1967;89:2874.

[33] Pedrosa P, Pomposo JA, Calahorra E, Ortega M. Macromolecules 1994;27:102.